Annual Report: Damage zones of the Elsinore and Superstition Hills Faults: Evidence of a moment-dependent bifurcation in off fault energy dissipation processes? (SCEC Award # 21043)

Principal Investigators:
W. Ashley Griffith, School of Earth Sciences, Ohio State University
Thomas Rockwell, Department of Geological Sciences, San Diego State University

1. Key Points:

- We proposed to conduct an initial test of the hypothesis that energy dissipation by inelastic off-fault deformation increases dramatically above Mw 6.6-6.8.
- To this end, we conducted field work in June 2021 and November 2021 to map fault damage zones, measure mesoscopic (outcrop-scale) fracture density and orientation data at varying distances from the fault core, and we collected oriented samples for thin section analysis of microstructure at similar positions. The bulk of the field work was conducted in November 2021 due to pandemic-related travel delays in early 2021, so we requested a one year no cost extension to complete our analysis.
- Initial results show that macroscopic and microscopic fracture density distribution are different within each damage zone.
  - In the Elsinore damage zone at Fossil Canyon, macroscopic damage is in the form of deformation band arrays. Deformation bands occur in several sets, but deformation band density does not decay with distance from the principal slip zone of the Elsinore fault. Instead, deformation bands form clusters around secondary faults within the damage zone. In contrast, at the Superstition Hills fault at Imler Road, macroscopic damage is in the form of discrete fractures, in some cases with minor normal offsets, that occur in one dominant set. Fracture density in these macroscopic damage zone fractures decays with distance from the fault.
  - We are currently conducting microstructural analysis of oriented damage zone samples, but preliminary inspection suggests that damage zone rocks from the Superstition Hills fault have undergone very little sub-grain fracturing at any distance from the fault, whereas subgrain fracture and shattering is prevalent in the damage zone of the Elsinore fault at Fossil Canyon.
- While work is ongoing, our preliminary interpretation is that deformation bands at Fossil Canyon are not related to recent seismogenic slip on the Elsinore fault and may have formed in response to longer term slip transfer between individual segments of the Elsinore fault. Damage zone fracturing and shattering at the sub-grain scale is, however, related to seismogenic slip, and this may constitute a non-negligible energy sink during seismic slip. In contrast, damage zone fracturing around the Superstition Hills fault at Imler Road is limited to macroscopic fractures and represents negligible off-fault energy dissipation.
- These observations, if they hold, are consistent with our original hypothesis that above a critical Mw transition (Mw 6.6 to 6.8) energy dissipation occurs increasingly by off fault deformation. We have proposed to continue this investigation at a location along the Southern San Andreas Fault in the 2022 SCEC collaboration plan.

2. Summary

Fault damage zones exert significant controls on strain localization, slip stability, coseismic rupture propagation, and interseismic stress accumulation and strength recovery. Velocity reductions in the damage zone have been shown to persist throughout the seismic cycle (e.g., Cochran et al., 2009, Qiu et al., 2020), and permanent damage zone size and intensity have been shown to scale with fault maturity (e.g., Savage and Brodsky, 2011; Faulkner et al., 2011; Scholz, 1987). Damage zones are the physical manifestation of feedbacks between processes related to fault slip and off-fault inelastic deformation. Some work has postulated that characteristics of the damage zone, such as the width and decay rate of fracture intensity, along seismogenic faults can be explained by inelastic deformation during seismic rupture (e.g., Johri et al., 2014a; Okubo et al., 2019), and at least some observations appear to support this idea (Johri et al., 2014b).

Interestingly, work from two completely different perspectives have arrived at the same suggestion that the nature of off-fault damage may depend on the magnitude of seismic energy release. Both approaches independently suggest that the extent of fault damage, and thus the amount of energy dissipated by brittle off-fault deformation, changes starkly above a moment magnitude threshold of ~Mw6.6-6.8. First, Nielsen *et al*. (2016) showed that fracture energy calculated as the work done during the frictional weakening process in experimental rotary shear tests (G_f) closely tracks the seismologically determined fracture energy from natural earthquakes (G) for events with slip between 1 cm and 1m, but for larger events G_f underestimates G (Figure 1). They ascribed this bifurcation between laboratory and natural earthquakes to energy dissipation due to inelastic off-fault yielding, which is expected to increase with increasing rupture size (e.g., Okubo et al., 2019; Andrews, 2005). The second observation comes from field observations along active strike slip faults in Southern California. Strain in southern California is partitioned among several subparallel fault strands, most prominently the Southern San Andreas, San Jacinto, and the Elsinore Fault Zones (e.g., Fialko, 2006). The most recent earthquake on the southernmost Elsinore Fault in the Coyote Mountains was approximately Mw 6.8, compared to Mw7.3 on the San Jacinto and M7.8 Fort Tejon earthquake on the South-Central San Andreas fault (Rockwell et al., 2019; Salisbury et al., 2012; Agnew and Sieh, 1978). Near the southern termination of the San Jacinto Fault zone, the Mw 6.6 1987 Superstition Hills earthquake ruptured the Superstition Hills fault. and appears to have been preceded by prior earthquakes of similar size and slip distribution (Hudnut and Sieh, 1989; Lindvall et al., 1989; Sharp et al., 1989). At the surface, as much as half of the observed surface slip occurred as after slip in the months after the mainshock. The damage zones where these faults cross similar lithologic units are markedly different.

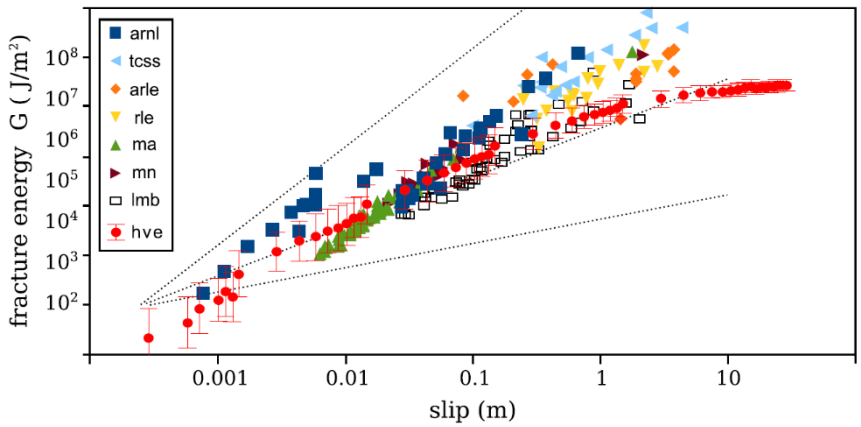

Figure 1: Experimental (high velocity rotary shear, hve), G_f, and seismological, G, estimates of fracture energy (from Nielsen et al., 2016). Red circles represent high velocity rotary shear experiments and all other datapoints are seismological estimate from natural earthquakes. Experimental and seismological estimates are roughly equivalent below 1 m of slip, but diverge above.

Some component of the energy dissipated during all earthquakes is expected to be partitioned into inelastic yielding off of the primary slip zone. As discussed above, the relative magnitude of this dissipated energy may vary as a function of earthquake magnitude, and *we posit that the key to understanding this relationship lies in examining the damage zone structure of active faults*. The damage zone structure of exhumed faults has received considerable attention in the literature, and more recently similar attention has been paid to active strands of the San Andreas and San Jacinto faults (e.g., Rempe et al., 2013; Wechsler et al., 2011; Dor et al., 2009; 2006a,b). The damage zones of these mature faults are complex, represent substantial seismic velocity reductions, and host abundant pulverized rocks. In contrast, the damage zone structure along the less mature Elsinore and Superstition Hills faults, which are the subject of 2021 SCEC Award #21043, are distinctly different. Along the Superstition Hills fault at Imler Road, where coseismic surface displacement during the 1987 Mw 6.6 event was approximately 20 cm (Lindvall et al., 1989; Sharp et al., 1989), the damage zone as viewed in sandstones of the Plio-Pleistocene Palm Springs group is largely absent, manifested only as narrow surface fissures extending out about 100m from the fault, with nearly undeformed sandstone outcrops exposed within centimeters from the rupture surface. The damage zone of the Elsinore Fault is well-exposed in the southern Coyote Mountains where the most recent ~Mw6.8 rupture had approximately 1.5m of surface slip. Here the damage zone displays some localized selective pulverization in crystalline igneous and metamorphic rocks. At the mouth of Fossil Canyon, sandstone of the Imperial Formation in the damage zone of the Elsinore Fault is poorly indurated and characterized by clusters of deformation bands reaching at least 200m from the fault.

The Elsinore (average slip rate ~ 3 mm/yr, Rockwell et al., 2019) and Superstition Hills (~3-6 mm/y: Hudnut and Sieh, 1989) host moderate earthquakes with Elsinore earthquakes larger than those on the Superstition Hills fault. These observations beg the question of whether there is a significant bifurcation in off fault deformation style and intensity in the Mw 6.6-6.8 range. In this work, we asked three complementary questions as part of the central hypothesis that coseismic off-fault damage increases dramatically for earthquakes among a critical moment magnitude threshold. First, ***how does fault maturity and local structure along the fault influence damage production***? Also, ***is the size of an earthquake a factor in pulverization, and***

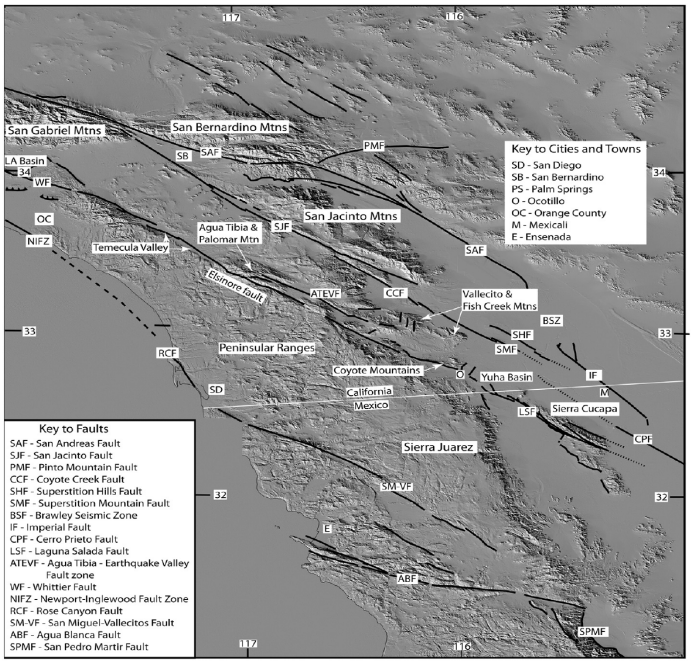

Figure 2: Map of the southern San Andreas fault system in southern California and northern Baja California (Rockwell et al., 2018). Elsinore fault passes through the Coyote Mountains, one proposed study site in this proposal. Superstition Hills Fault (SHF) to the northeast of the Coyote Mountains fault is the second study site.

where is that threshold? And perhaps most importantly, ***can we predict typical moment magnitudes or M_{max} values from fault zone architecture***? Given the short historical record of earthquakes, this last question is of huge potential importance in estimating seismic hazard on active faults in southern California and around the world.

Geologic Setting: The Elsinore fault is a NW-SE-trending right-lateral strike-slip fault that stretches from the Los Angeles basin through the Peninsular Ranges batholith southeast to nearly the US-Mexico border, where it steps right across Yuha Basin to the Laguna Salada fault (Fig. 2). From there, the fault system extends for at least another 120 km to the southeast into Baja California where it hosted twoM7.2 historical earthquakes in 1892 and 2010 (Mueller and Rockwell, 1995; Rockwell et al., 2015; Fletcher et al., 2014). The southern part of the Elsinore fault, the Coyote Mountain segment, bends to the left in a compressional jog and trends WNW-ESE, resulting in uplift of the Coyote Mountains. In the Coyote Mountains, the fault cuts through alluvial fans that have developed along the front of the range. The rocks exposed in the Coyote Mountains are dominantly pre-Cretaceous gneiss, schist, and marble with Mesozoic granitic rocks and pegmatites intruded into the Paleozoic host rock. Miocene Alverson andesite unconformably overlies the basement rock and is overlain by marine sedimentary rocks belonging to the Pliocene Imperial group and nonmarine rocks of the Plio-Pleistocene Palm Springs group. Based on offset alluvial fans along the Elsinore fault in the south-central Coyote Mountains, Rockwell et al. (2019) estimated the southernmost segment of the Elsinore fault has sustained a slip rate of 2.4±0.4mm/y for the past 60–70 ka and probably for the past 150 ka, slightly slower than rates of ~3mm/yr to the northwest.

The Superstition Hills are a low mountain range with the highest point of a few dozen meters above the Imperial Valley floor, southwest of the Salton Sea and northeast of the Coyote Mountains. The Superstition Hills are characterized by deeply incised topography, exposing two principal lithologies, weakly consolidated and deformed Pleistocene Brawley Formation, consisting of silty and clayey lake deposits with interbedded sandstones (Dibblee, 1954), overlain unconformably by Holocene unconsolidated alluvial deposits, dune sand, and lake bed deposits (Hudnut and Sieh, 1989). The Superstition Hills fault is a segmented right-lateral strike-slip fault (Jennings, 1994) that forms the southernmost strand of the San Jacinto Fault (Hudnut and Sieh, 1989). Total fault length is about 30km (Hudnut and Sieh, 1989). The Mw6.6 Superstition Hills earthquake occurred in the Imperial Valley on November 24, 1987, preceded

by about 12 hours by a M6.2 earthquake on the Elmore Ranch Fault, a northeast-striking cross-fault between the Brawley seismic zone and the Superstition Hills main fault. The Mw6.6 rupture nucleated in the north and ruptured unilaterally to the SE (Hudnut and Seeber, 1989). Maximum observed coseismic surface slip on the Superstition Hills fault was approximately 50cm. Postseismic slip distribution mirrored coseismic slip, with maximum slip of ~112cm (Sharp et al., 1989). Based on offsets of geomorphic features the size and slip distribution observed during the 1987 rupture appear to be similar to other recent ruptures on the Superstition Hills fault.

Little to no published data exists describing the damage zone structure of either the Elsinore Fault in the Coyote Mountains or the Superstition Hills Fault. In the Coyote Mountains, the damage zone is well-exposed and varies from fractured and deformation-banded, but otherwise coherent Imperial Formation sandstones (Figure 2) to intense brittle deformation localized around the active strand and extinct fault strands (Figure 3), and extremely localized pulverized leucogranites (Figure 4). Exposure of the damage zone in all lithologies is excellent due to incised valleys trending perpendicular to the active fault trace.

3. Completed Work

We identified eight outcrops at distances from 1m to 250m from the principal slip zone at each sites that afforded excellent exposure of damage zone fractures in sub-horizontal pavements. All data was collected in field notebooks at the FieldMove app in an iPad mini. At each outcrop, we recorded distance from the principal slip zone using a measuring tape, GPS-derived coordinates, bedding orientation, fracture orientations and mode, qualitative descriptions of structural observations, and slip vectors/slip sense when possible. At each outcrop, we used a high resolution digital camera to take photos of 1m x 1m outcrop sections using a square frame. Outcrop sizes varied between 2 m^2 and 13 m^2. Images were rectified and assembled into photomosaics. Using photomosaics we digitized fracture traces and imported vector graphics data from digital fracture maps into Matlab. Using the Matlab toolbox FracPaQ (Healy et al., 2017), we analyzed fracture orientation and density at each outcrop. Fracture density was conducted using the approach of Maulden et al. (2001), in which the fracture map is divided into N equal size scan circles. Fracture density is then calculated by counting the total number of fracture intersections with each circular scanline and dividing by circle scanline length. We determined density statistics by taking the mean and standard deviations from all scanline circles at each outcrop, omitting data from scanline circles that overlapped with cover material that obscured any part of the outcrop.

The Elsinore fault damage zone at Fossil Canyon, macroscopic damage is in the form of deformation band arrays. Deformation bands occur in several sets (e.g., Figure 3), but deformation band density does not decay with distance from the principal slip zone of the Elsinore fault (Figure 5A). Instead, deformation bands form clusters around secondary faults within the damage zone. In contrast, at the Superstition Hills fault at Imler Road, macroscopic damage is in the form of discrete fractures, in some cases with minor normal offsets, that occur in one dominant set (Figure 4). Fracture density in these macroscopic damage zone fractures decays with distance from the fault (Figure 5B).

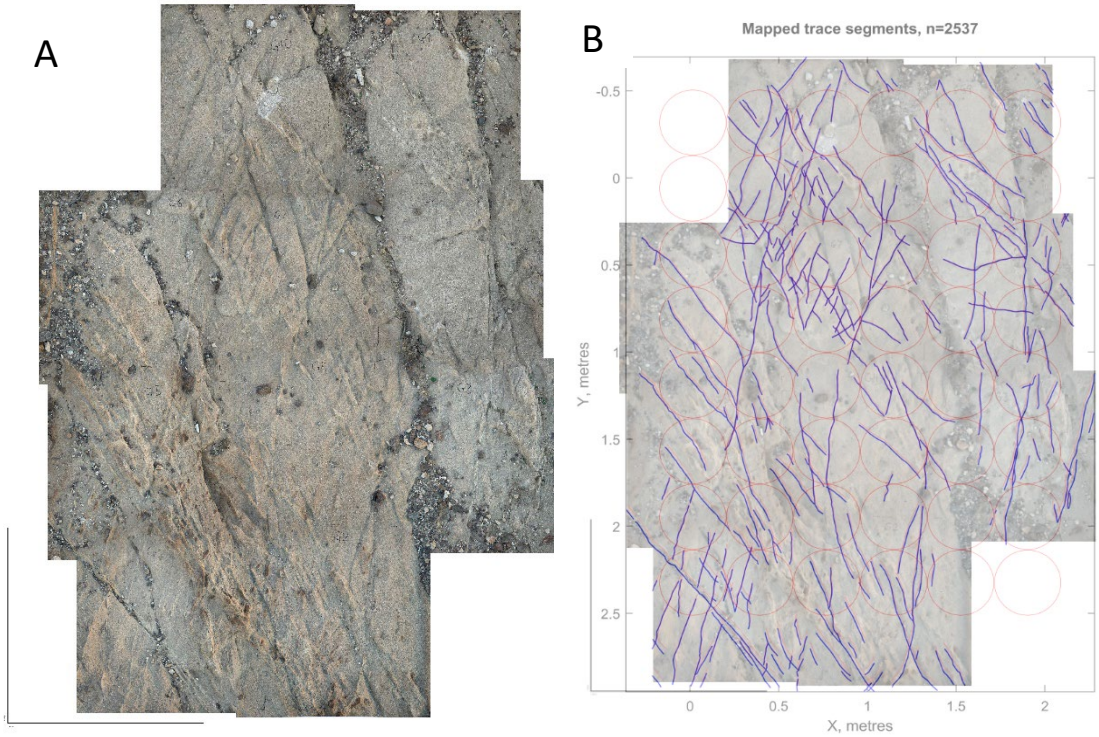

Figure 3: (A) Photomosaic of outcrop G at Fossil canyon in the Elsinore fault damage zone. Vertical and horizontal scale bars are 1 meter. (B) Interpreted fault map overlain by scan circles.

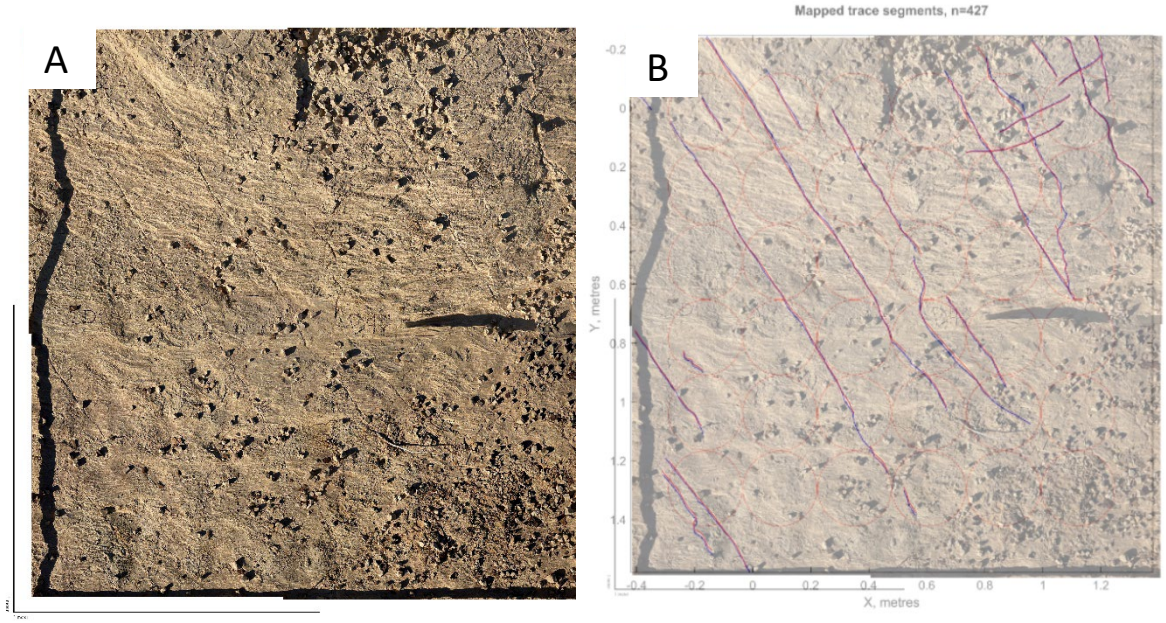

Figure 4: (A) Photomosaic of outcrop D at Imler Road in the Superstition Hills fault damage zone. Vertical and horizontal scale bars are 1 meter. (B) Interpreted fault map overlain by scan circles.

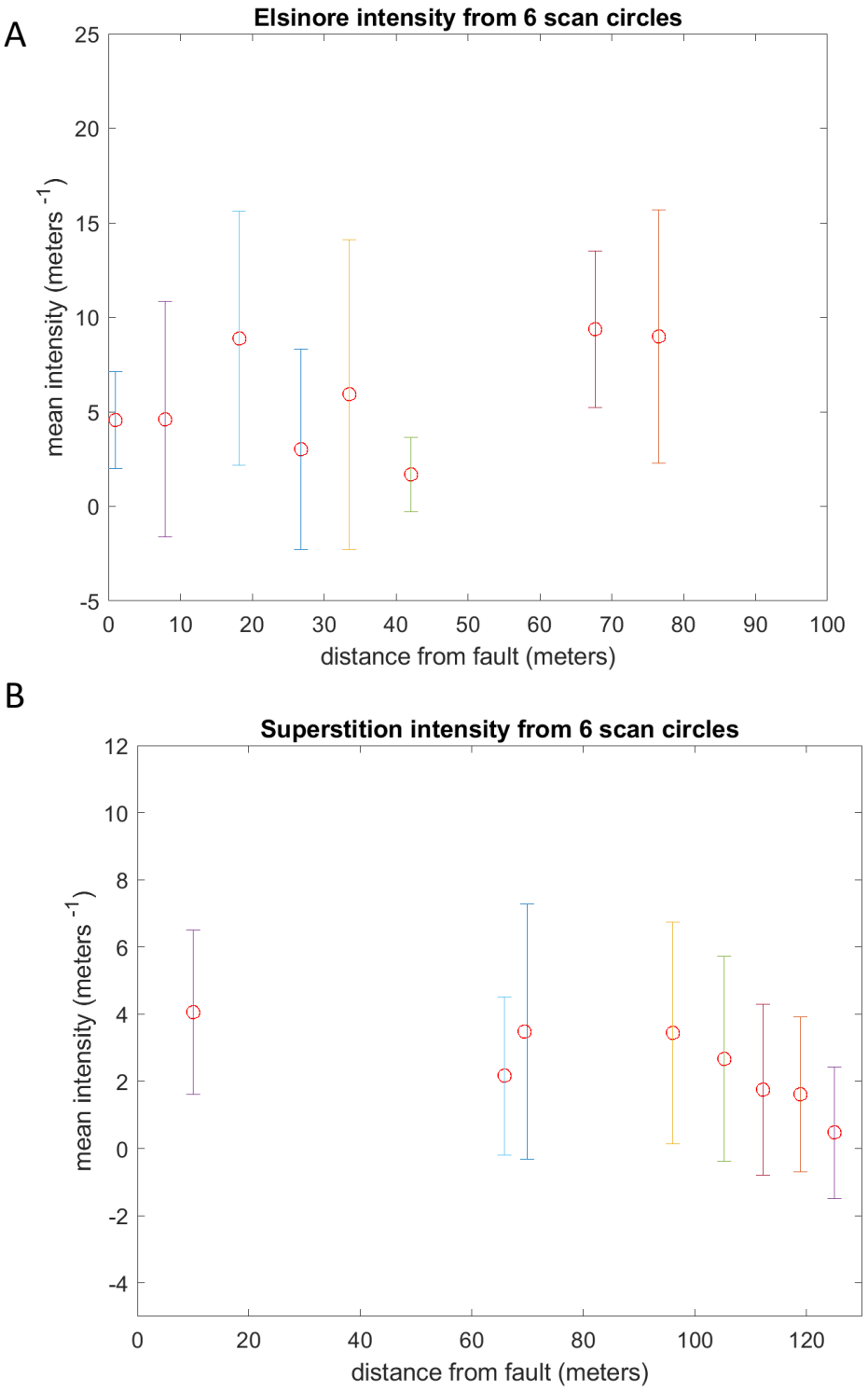

Figure 5: Mesoscopic fracture density as a function of distance from (A) the Elsinore fault as Fossil Canyon and (B) the Superstition Hills Fault at Imler Road.

4. Remaining Work

We are still in the process of processing fracture density and orientation data from additional outcrops. This data will be combined with data presented in Figure 5 and synthesized with microstructural data (below) to consider implications for our central hypothesis.

At most outcrops we also collected oriented samples. Because rocks are weakly indurated at both sites, we collected oriented samples by carving out blocks and encasing in optical grade epoxy resin. Encased blocks were transported back to Ohio State, where we vacuum empregnated the interior of each block, and then cut samples into oriented slabs for thin sections in both vertical and horizontal orientations. Some example thin sections are shown in Figure 6. We are currently analyzing microstructural rock deformation following methods outlined by Dor et al. (2009).

In thin section, rocks collected within 1-2m from the principal slip zone of the Superstition Hills damage zone at Imler Rd are well-cemented and display no deformation at the subgrain scale (Figure 6A). Most damage zone rocks there are very poorly indurated, and we are still awaiting thin sections of these rocks, however preliminary investigation with hand lens suggests there is no subgrain deformation. In the Elsinore damage zone at Fossil Canyon, in contrast, poor induration is caused in large part by extensive subgrain fractures up to 10s of meters from the fault (Figure 6B), and initial results indicate that this damage decays substantially approximately 100m from the fault. For comparison, work by Dor et al. (2009) in sedimentary rocks of the Juniper Hills and Hungry Valley Formations in the Mojave section of the San Andreas fault show extensive subgrain fracturing, in some places resembling pulverized rock textures at least 125m from the main fault (Figure 6C). This section of the fault has experienced a recurrence interval of 105 years (full range 31-165 years) and a mean slip-per-event of 3.2m (full range 0.7-7 m).

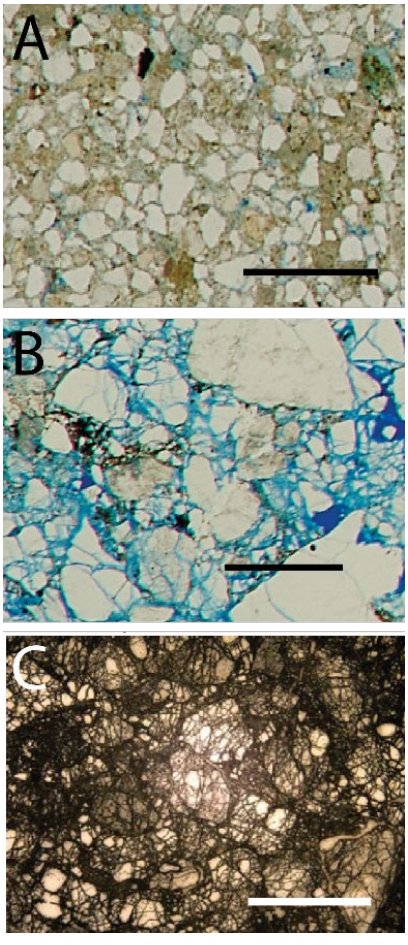

Figure 6: Microstructural character of sandstones in the damage zones of the (A) Superstition Hills Fault at Imler Rd (~20 cm of coseismic surface slip), (B) Elsinore Fault at Fossil Canyon (~1.5 m of coseismic surface slip), and (C) the Mojave section of the San Andreas Fault in the Hungry Valley Formation (0.7 to 7mm of coseismic surface slip) (image from Dor et al., 2009). Historical or paleoseismic earthquakes increase in size from (A) to (C). Samples in (A) and (B) were collected less than 1m from the fault core, whereas the sample shown in (C) was collected 125 m from the fault core. Scale bar in all thin sections is 1 mm.

5. References

Agnew, D. C., & Sieh, K. E. (1978). A documentary study of the felt effects of the great California earthquake of 1857. *Bulletin of the Seismological Society of America*, *68*(6), 1717–1729.

Andrews, D. J. (2005). Rupture dynamics with energy loss outside the slip zone. *Journal of Geophysical Research: Solid Earth*, *110*(B1).

Cochran, E. S., Li, Y. G., Shearer, P. M., Barbot, S., Fialko, Y., & Vidale, J. E. (2009). Seismic and geodetic evidence for extensive, long-lived fault damage zones. *Geology*, *37*(4), 315-318.

Dibblee Jr, T. W. (1954). Geology of the Imperial Valley region, California. *Geology of southern California: California Division of Mines Bulletin*, *170*, 21-28.

Dor, O., Ben-Zion, Y., Rockwell, T. K., & Brune, J. (2006a). Pulverized rocks in the Mojave section of the San Andreas Fault Zone. *Earth and Planetary Science Letters*, *245*(3-4), 642-654.

Dor, O., Rockwell, T. K., & Ben-Zion, Y. (2006b). Geological observations of damage asymmetry in the structure of the San Jacinto, San Andreas and Punchbowl faults in Southern California: a possible indicator for preferred rupture propagation direction. *Pure and Applied Geophysics*, *163*(2-3), 301-349.

Dor, O., Chester, J. S., Ben-Zion, Y., Brune, J. N., & Rockwell, T. K. (2009). Characterization of damage in sandstones along the Mojave section of the San Andreas Fault: Implications for the shallow extent of damage generation. In *Mechanics, Structure and Evolution of Fault Zones* (pp. 1747-1773). Birkhäuser Basel.

Faulkner, D. R., Mitchell, T. M., Jensen, E., & Cembrano, J. (2011). Scaling of fault damage zones with displacement and the implications for fault growth processes. *Journal of Geophysical Research: Solid Earth*, *116*(B5).

Fialko, Y. (2006). Interseismic strain accumulation and the earthquake potential on the southern San Andreas fault system. *Nature*, *441*(7096), 968-971.

Fletcher, J. M., Teran, O. J., Rockwell, T. K., Oskin, M. E., Hudnut, K. W., Mueller, K. J., Spelz, R. M., Akciz, S. O., Masana, E., Faneros, G., Fielding, E. J., Leprince, S., Morelan, A. E., Stock, J., Lynch, D. K., Elliott, A. J., Gold, P., Liu-Zeng, J., González-Ortega, A., … González-García, J. (2014). Assembly of a large earthquake from a complex fault system: Surface rupture kinematics of the 4 April 2010 El Mayor–Cucapah (Mexico) Mw 7.2 earthquake. *Geosphere*, *10*(4), 797–827.

Healy, D., Rizzo, R., Cornwell, D., Farrell, N., Watkins, H., Timms, N., Gomez-Rivas, E., & Smith, M. (2016). FracPaQ: A MATLAB™ toolbox for the quantification of fracture patterns. *Journal of Structural Geology*, *95*.

Hudnut, K. W., Seeber, L., & Pacheco, J. (1989). Cross-fault triggering in the November 1987 Superstition Hills Earthquake sequence, southern California. Geophysical Research Letter, 16 (2), 199-202. https://doi.org/10.1029/gl016i002p00199

Hudnut, K. W., K. E. Sieh (1989); Behavior of the Superstition Hills fault during the past 330 years. *Bulletin of the Seismological Society of America*; 79 (2): 304–329.

Jennings, C.W., and Bryant, W.A., 2010, Fault activity map of California: California Geological Survey Geologic Data Map No. 6, map scale 1:750,000.

Johri, M., Dunham, E. M., Zoback, M. D., & Fang, Z. (2014a). Predicting fault damage zones by modeling dynamic rupture propagation and comparison with field observations. *Journal of Geophysical Research: Solid Earth*, *119*(2), 1251-1272.

Johri, M., Zoback, M., & Hennings, P. (2014b). A scaling law to characterize fault-damage zones at reservoir depths. *AAPG Bulletin*, *98*, 2057–2079.

Kindred, C. A., Griffith, W. A., & Rockwell, T. K. (2020, 08). Role of confinement in coseismic pulverization of sediments: testing the rock record of rupture directivity on the San Jacinto fault . Poster Presentation at 2020 SCEC Annual Meeting.

Lindvall, S. C., Rockwell, T. K., & Hudnut, K. W. (1989). Evidence for prehistoric earthquakes on the Superstition Hills fault from offset geomorphic features. *Bulletin of the Seismological Society of America*, *79*(2), 342-361.

Mauldon, M., Dunne, W.M. & Rohrbaugh, M.B. (2001). Circular scanlines and circular windows: new tools for characterizing the geometry of fracture traces. *Journal of Structural Geology*, *23*(2), pp.247-258.

Mueller, K. J., & Rockwell, T. K. (1995). Late quaternary activity of the Laguna Salada fault in northern Baja California, Mexico. *Geological Society of America Bulletin*, *107*(1), 8-18.

Nielsen, S., Spagnuolo, E., Violay, M., Smith, S., Di Toro, G., & Bistacchi, A. (2016). G: Fracture energy, friction and dissipation in earthquakes. *Journal of Seismology*, *20*(4), 1187-1205.

Okubo, K., Bhat, H.S., Rougier, E., Marty, S., Schubnel, A., Lei, Z., Knight, E.E. and Klinger, Y., 2019. Dynamics, Radiation, and Overall Energy Budget of Earthquake Rupture With Coseismic Off-Fault Damage. *Journal of Geophysical Research: Solid Earth*, *124*(11), pp.11771-11801.

Ostermeijer, G. A., Mitchell, T. M., Aben, F. M., Dorsey, M. T., Browning, J., Rockwell, T. K., Fletcher, J. M., & Ostermeijer, F. (2020). Damage zone heterogeneity on seismogenic faults in crystalline rock; a field study of the Borrego Fault, Baja California. *Journal of Structural Geology*, *137*, 104016.

Qiu, H., Hillers, G., & Ben-Zion, Y. (2020). Temporal changes of seismic velocities in the San Jacinto Fault zone associated with the 2016 M w 5.2 Borrego Springs earthquake. *Geophysical Journal International*, *220*(3), 1536-1554.

Rempe, M., Mitchell, T., Renner, J., Nippress, S., Ben-Zion, Y., & Rockwell, T. (2013). Damage and seismic velocity structure of pulverized rocks near the San Andreas Fault. *Journal of Geophysical Research: Solid Earth*, *118*(6), 2813-2831.

Rockwell, T. K., Fletcher, J. M., Teran, O. J., Hernandez, A. P., Mueller, K. J., Salisbury, J. B., ... & Štěpančíková, P. (2015). Reassessment of the 1892 Laguna Salada Earthquake: Fault Kinematics and Rupture Patterns. *Bulletin of the Seismological Society of America*, *105*(6), 2885-2893.

Rockwell, T. K., Masana, E., Sharp, W. D., Štěpančíková, P., Ferrater, M., & Mertz-Kraus, R. (2019). Late Quaternary slip rates for the southern Elsinore fault in the Coyote Mountains, southern

California from analysis of alluvial fan landforms and clast provenance, soils, and U-series ages of pedogenic carbonate. *Geomorphology*, *326*, 68-89.

Salisbury, J.B., Rockwell, T.K., Middleton, T.J., and Hudnut, K.W. (2012). LiDAR and Field Observations of Slip Distribution for the Most Recent Surface Ruptures Along the Central San Jacinto Fault. Bulletin of the Seismological Society of America, v. 102, no. 2, p. 598-619. doi: 10.1785/0120110068.

Savage, H. M., & Brodsky, E. E. (2011). Collateral damage: Evolution with displacement of fracture distribution and secondary fault strands in fault damage zones. *Journal of Geophysical Research: Solid Earth*, *116*(B3).

Scholz, C. H. (1987). Wear and gouge formation in brittle faulting. *Geology*, *15*(6), 493-495.

Sharp, R. V. (1989). Surface faulting along the Superstition Hills fault zone and nearby faults associated with the earthquakes of 24 November 1987. *Bulletin of the Seismological Society of America*, *79*(2), 252–281. http://pubs.er.usgs.gov/publication/70015826

Wechsler, N., Allen, E. E., Rockwell, T. K., Girty, G., Chester, J. S., & Ben-Zion, Y. (2011). Characterization of pulverized granitoids in a shallow core along the San Andreas Fault, Littlerock, CA. *Geophysical Journal International*, *186*(2), 401-417.